

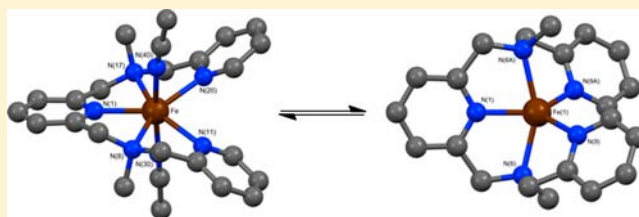
Coordination Equilibria Between Seven- and Five-coordinate Iron(II) Complexes

Michaela Grau, Jason England, Rafael Torres Martin de Rosales, Henry S. Rzepa, Andrew J. P. White, and George J. P. Britovsek*

Department of Chemistry, Imperial College London, Exhibition Road, London, SW7 2AY, U.K.

S Supporting Information

ABSTRACT: Octahedral, tetrahedral, and square planar geometries are the most often encountered coordination geometries for transition metal complexes. In certain cases, coordination equilibria can exist between different geometries, such as between six- and four-coordinate geometries in nickel(II) complexes, which were discovered half a century ago. Here, we present the first examples of a seven-five coordination equilibrium. Extensive spectroscopic studies in solution have provided evidence for a dynamic equilibrium between two iron(II) complexes, one with a seven-coordinate pentagonal bipyramidal geometry and one with a five-coordinate trigonal bipyramidal geometry.



Extensive spectroscopic studies in solution have provided evidence for a dynamic equilibrium between two iron(II) complexes, one with a seven-coordinate pentagonal bipyramidal geometry and one with a five-coordinate trigonal bipyramidal geometry.

INTRODUCTION

One century ago, Alfred Werner was awarded the 1913 Nobel Prize in Chemistry for his pioneering work on the elucidation of the structure of metal complexes—the inception of inorganic coordination chemistry. Millions of different transition metal complexes are known today, of which more than 300,000 have been structurally characterized. Metal complexes have distinct geometries and the *coordination number*, as defined by Werner, can vary between 1 and 12.¹ Single crystal analysis techniques provide important information about the coordination behavior of metal complexes in the solid state. In solution however, coordination geometries can be fluxional, and this can be investigated by spectroscopic techniques such as NMR and UV–vis spectroscopy. In certain cases, metal complexes with different geometries can be in equilibrium, and this requires variable temperature (VT) or pressure (VP) measurements to characterize their dynamic coordination behavior.² A textbook example is the coordination equilibrium between trigonal bipyramidal (*TBPY-5*) and square pyramidal (*SPY-5*) geometries in five-coordinate complexes (Berry pseudorotation).^{3,4}

During the 1960s, coordination equilibria in solution between square planar (*SP-4*) and tetrahedral (*T-4*) geometries of four-coordinate nickel(II) complexes were extensively investigated, notably by Holm and Sacconi and later by Elias and Fukuda.^{5–8} Ligands can also dissociate, resulting in equilibria between complexes with different coordination numbers, because of either loss or gain of *one* ligand or sometimes *two* ligands in rapid succession. The two axial ligands in six-coordinate octahedral (*OC-6*) complexes can dissociate to give four-coordinate square planar complexes in the case of nickel(II) (*OC-6/SP-4* equilibrium),^{9–11} or tetrahedral complexes in the case of cobalt(II) (*OC-6/T-4* equilibrium).¹² For some nickel(II) complexes, equilibria between all three geometries octahedral-planar-tetrahedral

(*OC-6/SP-4/T-4* equilibrium) have been observed, as illustrated in Figure 1 (top).^{13,14} The *OC-6/SP-4* and *SP-4/T-4* coordination equilibria are accompanied by a change in spin state ($\Delta S = 1$) of the nickel(II) center. Evidence for the existence of these coordination and spin equilibria as well as their thermodynamic and kinetic parameters have been obtained by VT NMR and UV–vis spectroscopy, magnetic susceptibility measurements, and kinetic studies.^{11,15,16} Mechanistic studies have shown that the “slow” loss of one ligand from the kinetically inert octahedral complexes is followed by an extremely rapid loss of the other ligand, such that five-coordinate intermediates are rarely observed.^{7,17}

The question arises whether coordination equilibria, similar to the 6–4 equilibrium, could exist between other geometries? By strict analogy, one could propose a 7–5 equilibrium as illustrated in Figure 1 (bottom). To the best of our knowledge, such an equilibrium has never been reported. Upon loss of two axial ligands from a seven-coordinate complex with pentagonal bipyramidal coordination geometry (*PBPY-7*), a complex with pentagonal planar geometry (*PP-5*) would be obtained, at least in theory. In practice, this geometry is only known for certain main group compounds and is generally believed to be too unstable to be observed for transition metal complexes.^{18,19} The pentagonal planar intermediate could rearrange to a trigonal bipyramidal geometry (*TBPY-5*) by moving two ligands into axial positions. Further extrapolation to 8–6 or 5–3 coordination equilibria could also be envisaged.

We present here the first example of a coordination equilibrium between a seven-coordinate and a five-coordinate iron(II) complex. The dynamic behavior of metal complexes in solution is of fundamental importance for the understanding of

Received: June 4, 2013

Published: October 10, 2013



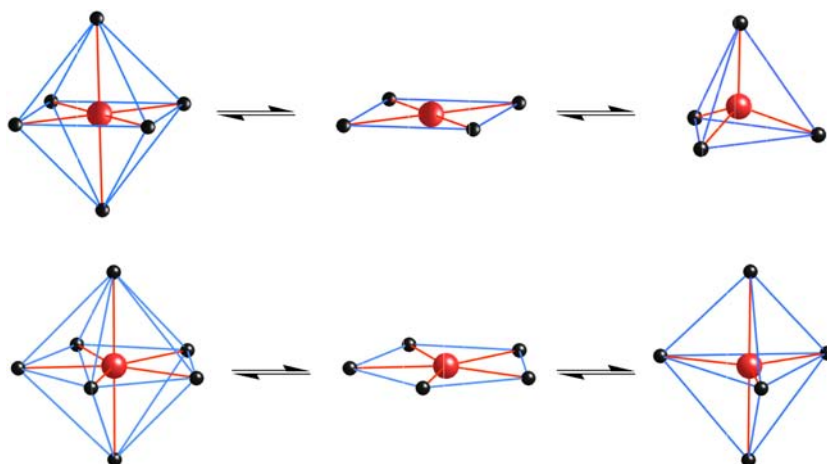


Figure 1. Analogous coordination equilibria between octahedral, square planar, and tetrahedral geometries (*OC-6/SP-4/T-4*) (top) and between pentagonal bipyramidal, pentagonal planar, and trigonal bipyramidal geometries (*PBPY-7/PP-5/TBPY-5*) (bottom).

their activity in chemical, catalytic, and biological processes. The discovery of this new 7–5 coordination equilibrium could have important consequences for the study of metal complexes in solution, in particular for metallo-enzymes, where spin and coordination equilibria are often essential features of their mode of action. Considering iron's prominent role in metallo-enzymes and in oxidation catalysis, the coordination equilibrium shown here could be present in other metal complexes, in particular where pentadentate ligands are involved, as for example, in the anticancer drug bleomycin,²⁰ or in functional mimics for superoxide dismutases.^{21,22}

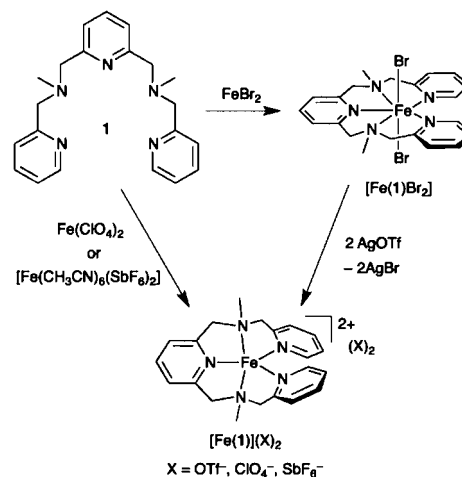
RESULTS

Synthesis of Ligands and Iron Complexes. The linear pentadentate ligand 2,6-bis[(methyl(2-pyridylmethyl)amino)-N-methyl]pyridine **1** was synthesized in a one-pot synthesis in 90% yield from 2,6-diformylpyridine and methyl(2-pyridylmethyl)amine using Na[B(OAc)₃H] as the reducing agent (see Supporting Information). The synthesis and application of the N-Methyl ligand **1** have not been reported so far, although there are several reports on the related N–H ligand and its coordination chemistry.^{23–25} A series of iron(II) complexes [Fe(**1**)(CH₃CN)₂](SbF₆)₂, [Fe(**1**)(CH₃CN)₂](ClO₄)₂, and [Fe(**1**)Br₂] has been prepared by reacting **1** with the relevant metal precursor in acetonitrile (see Scheme 1). For the synthesis of the bis(triflate) iron(II) complex of ligand **1**, the bromo ligands in complex [Fe(**1**)Br₂] were exchanged with AgOTf.

Complex [Fe(**1**)Br₂] was crystallized from an acetonitrile/diethyl ether solution at room temperature, and the solid state structure revealed a seven-coordinate iron(II) complex with a pentagonal bipyramidal (*PBPY-7*) geometry (see Figure 2, left). The FeN₅ pentagonal equatorial plane is slightly distorted with the two amino nitrogens N(8) and N(17) lying about 0.52 and 0.53 Å “below” and “above” the Fe(N_{pyr})₃ plane. The plane of the central pyridyl ring is twisted with respect to the Fe(N_{pyr})₃ plane by about 31° about the Fe(1)–N(1) bond. The distortion is probably due to Jahn–Teller effects, further removing the degeneracy of the asymmetrically occupied lowest d_{xz} and d_{yz} orbitals.

A seven-coordinate *PBPY-7* geometry was also obtained for the bis(acetonitrile) complex [Fe(**1**)(CH₃CN)₂](ClO₄)₂, which was crystallized from an acetonitrile/diethyl ether

Scheme 1. Syntheses of Iron(II) Complexes



solution at room temperature (Figure 2, middle). The ligand geometry is little different to that seen in the neutral dibromo complex. The amino nitrogens N(8) and N(17) lie about 0.64 and 0.65 Å “below” and “above” the Fe(N_{pyr})₃ plane, and the central pyridine ring plane is twisted about the Fe–N(1) bond by about 36° with respect to the Fe(N_{pyr})₃ plane.

While seven-coordinate geometries are found across the transition series,²⁶ they are far less common than octahedral metal complexes and account for only approximately 2% of all metal complexes and less than 1% of all iron complexes.^{27,28} The first seven-coordinate iron(II) complex with *PBPY-7* geometry, reported by Palenik in 1973, featured a linear pentadentate ligand with a N₃O₂ donor set.²⁹ Since then, other seven-coordinate iron(II) complexes have been reported with linear or macrocyclic pentadentate ligands and two monodentate ligands in the axial positions.²⁸ Seven-coordinate complexes are generally high spin, although spin transition has been observed in one example.³⁰

When complex [Fe(**1**)](OTf)₂ was crystallized from a dichloromethane/pentane solution at room temperature, a five-coordinate complex was obtained with a distorted trigonal bipyramidal (*TBPY-5*) geometry and a τ -index of 0.89,³¹ whereby N(6) and N(6A) occupy the axial sites (Figure 2, right). The complex has C₂ symmetry about an axis that passes through N(1) and Fe(1), and consequently the Fe(N_{pyr})₃

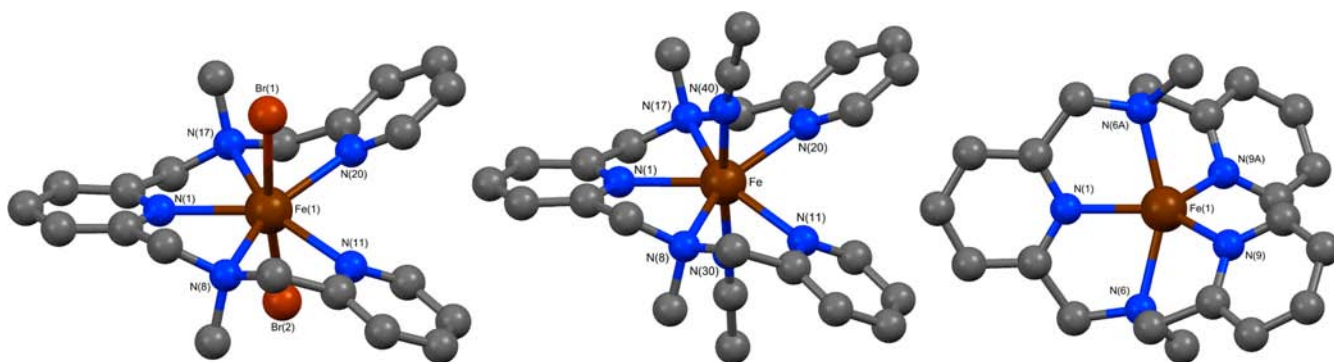


Figure 2. Molecular structures of $[\text{Fe}(\mathbf{1})\text{Br}_2]$, $[\text{Fe}(\mathbf{1})(\text{CH}_3\text{CN})_2](\text{ClO}_4)_2$, and $[\text{Fe}(\mathbf{1})](\text{OTf})_2$. Noncoordinating perchlorate and triflate counterions as well as all hydrogen atoms have been omitted for clarity.

equatorial plane is perfectly flat. The two triflate anions are located “above” and “below” the iron center and the central pyridine ring, such that the closest $\text{O}\cdots\text{Fe}$ and $\text{F}\cdots\pi$ contacts are both approximately 3.23 \AA , too far to be considered as bonding interactions. In the two seven-coordinate complexes, the plane of the central pyridine ring is twisted with respect to the equatorial $\text{Fe}(\text{N}_{\text{pyr}})_3$ plane by about 31° and 36° respectively, while in the five-coordinate complex $[\text{Fe}(\mathbf{1})](\text{OTf})_2$ this twist is about 72° . For all complexes, the amino nitrogens become chiral upon coordination, and in all cases a racemic mixture of the (*S,S*) and (*R,R*) diastereomers is obtained. The *meso*-form with (*S**, *R**) configuration, where both methyl substituents point in the same direction, is not observed, probably because of steric repulsion between the two outer pyridine groups. The conformational change of the ligand from a seven- to a five-coordinate geometry can be viewed as the three pyridyl nitrogen atoms staying in one place, while a twist of the central pyridine ring about the $\text{N}(\mathbf{1})\text{--Fe}$ axis moves the amino nitrogens from equatorial to axial sites. The observation of different coordination geometries in the solid state for complexes containing the same metal and ligand, prompted further investigation of the behavior in solution by NMR and UV–vis spectroscopy.

NMR Spectroscopy. The paramagnetic ^1H NMR spectrum of $[\text{Fe}(\mathbf{1})](\text{OTf})_2$ in CD_3CN at room temperature shows 22 signals, covering a chemical shift range from $+150$ to -10 ppm (see Figure 3). Upon heating, the spectrum simplifies gradually to 11 signals at 343 K (labeled I–XI), whereas cooling to 233 K results in a different set of 11 signals (*I'*–*XI'*). The two sets of 11 signals suggest the presence of two different iron(II) complexes with C_2 - or C_s -symmetry that interconvert slowly on the NMR time scale. The ^{19}F -NMR spectrum in CD_3CN shows a single sharp resonance at -78 ppm at low temperature (233 K), which changes to -72 ppm at 343 K (see Supporting Information, Figure S6). These chemical shift values are typical for non-coordinated triflate anions, and the small change is due to the change in temperature. Unlike $[\text{Fe}(\mathbf{1})](\text{OTf})_2$, the ^1H NMR spectrum of $[\text{Fe}(\mathbf{1})\text{Br}_2]$ in CD_3CN displays only one set of 11 signals over the entire temperature range (see Supporting Information, Figure S5).

The observations indicate a dynamic equilibrium between a seven-coordinate bis(acetonitrile) complex $[\text{Fe}(\mathbf{1})(\text{CD}_3\text{CN})_2](\text{OTf})_2$ at low temperature (<243 K) and a five-coordinate complex $[\text{Fe}(\mathbf{1})](\text{OTf})_2$ at high temperature (>333 K), as shown in eq 1. The VT ^1H NMR spectra for $[\text{Fe}(\mathbf{1})](\text{SbF}_6)_2$ and $[\text{Fe}(\mathbf{1})](\text{ClO}_4)_2$ in CD_3CN are identical to those for $[\text{Fe}(\mathbf{1})](\text{OTf})_2$ (see Supporting Information, Figures S10 and

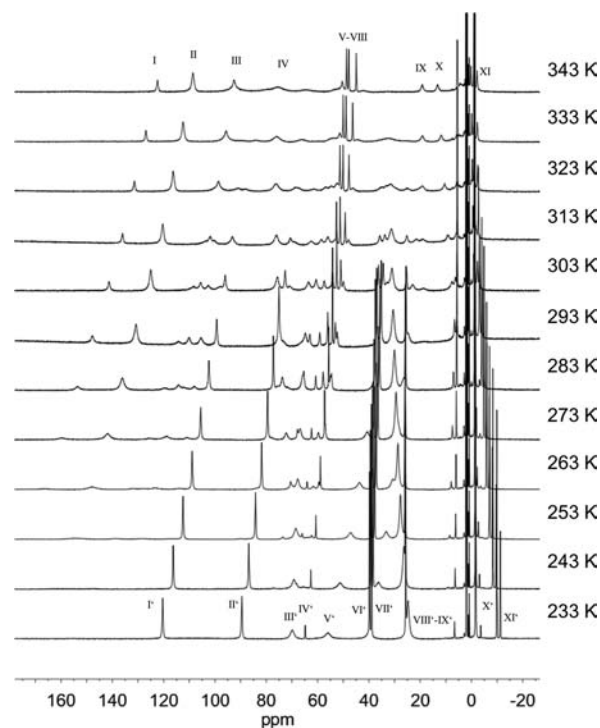
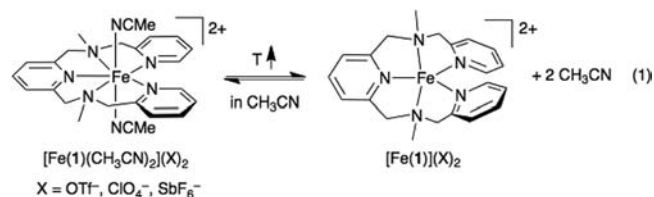


Figure 3. VT ^1H NMR spectra in the temperature range 233 to 343 K for $[\text{Fe}(\mathbf{1})](\text{OTf})_2$ in CD_3CN .



S12), which shows that the noncoordinating anions do not affect the 7–5 equilibrium in acetonitrile. The ^{19}F NMR spectrum of $[\text{Fe}(\mathbf{1})](\text{SbF}_6)_2$ in CD_3CN shows the SbF_6^- anions and also in this case, there is no interaction with the iron(II) center over the temperature range 233–343 K and this complex is therefore assumed to exist as $[\text{Fe}(\mathbf{1})(\text{CD}_3\text{CN})_2]^{2+}$ at low temperature and as $[\text{Fe}(\mathbf{1})]^{2+}$ at high temperature (see Supporting Information, Figure S11).

The relative amounts of each complex $[\text{Fe}(\mathbf{1})(\text{CD}_3\text{CN})_2]^{2+}$ and $[\text{Fe}(\mathbf{1})]^{2+}$ at different temperatures (273–313 K) have been determined by integration of the ^1H NMR spectra, and

the results are plotted in Figure 4, which shows that the five-coordinated complex becomes favored at temperatures above

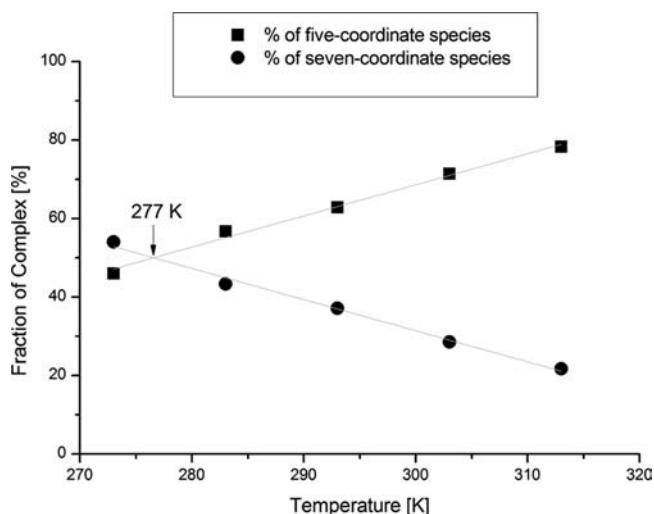


Figure 4. Fraction of the complexes $[\text{Fe}(\mathbf{1})]^{2+}$ (square) and $[\text{Fe}(\mathbf{1})(\text{CD}_3\text{CN})_2]^{2+}$ (round) in % as a function of temperature in CD_3CN , determined by integration of the ^1H NMR signals.

277 K. The equilibrium constant $K = [\text{Fe}(\mathbf{1})]^{2+} \cdot [\text{CD}_3\text{CN}]^2 / [\text{Fe}(\mathbf{1})(\text{CD}_3\text{CN})_2]^{2+}$ for the reaction in eq 1 was calculated at different temperatures and the van 't Hoff plot of $\ln K$ versus $1/T$ resulted in $\Delta H^\circ = 25.1 \pm 1.1 \text{ kJ mol}^{-1}$ and $\Delta S^\circ = 91 \pm 4 \text{ J K}^{-1} \text{ mol}^{-1}$ (see Supporting Information, Figure S16). At 298 K, the equilibrium constant $K = 780 \text{ M}^2$ or $K' = [\text{Fe}(\mathbf{1})]^{2+} / [\text{Fe}(\mathbf{1})(\text{CD}_3\text{CN})_2]^{2+} = 2.1$ (whereby $K = K' \cdot [\text{CD}_3\text{CN}]^2$ and $[\text{CD}_3\text{CN}] = 19.2 \text{ M}$ at 298 K). The loss of acetonitrile from the seven-coordinate complex is an endothermic process of breaking two axial Fe–N bonds, and the equilibrium is driven by entropic effects resulting in $\Delta G^\circ = -2.0 \pm 2.3 \text{ kJ mol}^{-1}$ at 298 K (see Supporting Information, Figure S17). These thermodynamic data can be compared to the OC-6/SP-4 equilibrium between $[\text{Ni}(\text{cyclam})(\text{CH}_3\text{CN})_2]^{2+}$ and $[\text{Ni}(\text{cyclam})]^{2+}$ with values of $\Delta H^\circ = 18.4 \text{ kJ mol}^{-1}$ and $\Delta S^\circ = 52 \text{ J K}^{-1} \text{ mol}^{-1}$ (determined by VT UV–vis spectroscopy).¹¹ The lower values in this case are probably due to the required spin pairing from the high spin (HS) octahedral complex to a low spin (LS) square planar complex.

Density functional theory (DFT) calculations have been carried out at the $\omega\text{B97X-D}$ level using 6-31G(d) basis sets for all atoms, except Fe, which was 6-31G(2df) for a quintet spin state, and including a continuum solvation correction for acetonitrile (see Supporting Information for details).³² The optimized seven-coordinate geometries were obtained for both complexes $[\text{Fe}(\mathbf{1})(\text{OTf})_2]$ and $[\text{Fe}(\mathbf{1})(\text{CH}_3\text{CN})_2](\text{OTf})_2$. Complex $[\text{Fe}(\mathbf{1})(\text{CH}_3\text{CN})_2](\text{OTf})_2$ in acetonitrile as the solvent medium shows a close proximity of the two triflate anions to the dicationic complex, probably because of electrostatic and H-bonding interactions (Supporting Information, Figure S20). Removal of the acetonitrile nitrile ligands resulted in the optimized geometry for the bis(triflate) complex $[\text{Fe}(\mathbf{1})(\text{OTf})_2]$ (Supporting Information, Figure S21). Attempts to calculate the five-coordinate complex $[\text{Fe}(\mathbf{1})](\text{OTf})_2$ with two noncoordinating triflate anions always resulted in coordination of the triflate anions to give the seven-coordinate complex $[\text{Fe}(\mathbf{1})(\text{OTf})_2]$, which highlights the intrinsic difficulties associated with calculating ion pairs. The difference

in free energies between the two seven-coordinate complexes $[\text{Fe}(\mathbf{1})(\text{CH}_3\text{CN})_2](\text{OTf})_2$ and $[\text{Fe}(\mathbf{1})(\text{OTf})_2]$ (and two CH_3CN) was calculated as $\Delta G^\circ = -40 \text{ kJ mol}^{-1}$.

In the noncoordinating solvent CD_2Cl_2 , the ^1H NMR spectra of $[\text{Fe}(\mathbf{1})](\text{OTf})_2$, measured over the temperature range from 203–303 K (see Supporting Information, Figure S7), are similar to those measured in CD_3CN shown in Figure 3. The ^{19}F NMR spectrum in CD_2Cl_2 at low temperature (203 K in Figure 5) shows a single peak at +62 ppm. This large downfield

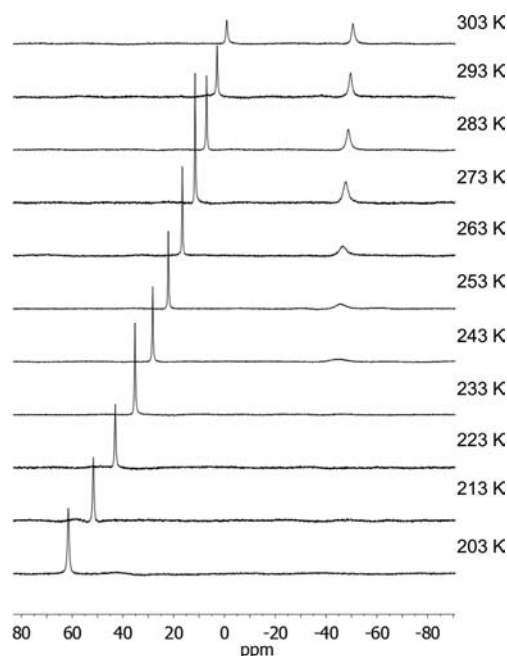


Figure 5. VT ^{19}F -NMR spectra in the temperature range 203 to 303 K for $[\text{Fe}(\mathbf{1})](\text{OTf})_2$ in CD_2Cl_2 .

shift indicates that the triflate anions are coordinated to the iron(II) center to give $[\text{Fe}(\mathbf{1})(\text{OTf})_2]$. Increasing the temperature results in a shift of this signal because of Curie behavior and, more importantly, a gradual decrease in intensity. Above 243 K, a second peak emerges at -45 ppm , which is assigned to $[\text{Fe}(\mathbf{1})](\text{OTf})_2$ with non-coordinated triflate. The ratio between coordinated versus non-coordinated triflate changes gradually and equal amounts of seven- and five-coordinate species are obtained at 273 K (see Supporting Information, Figure S8).

To increase the temperature above 303 K, the NMR spectra of complex $[\text{Fe}(\mathbf{1})](\text{OTf})_2$ were measured in $1,2\text{-C}_2\text{D}_4\text{Cl}_2$ (bp. = 357 K). The ^{19}F NMR spectra in Figure 6 show that the ratio of coordinated to non-coordinated triflate changes from 2:1 at 243 K to become exclusively non-coordinated triflate at 343 K with a chemical shift of -55 ppm . The ^1H NMR spectrum in $1,2\text{-C}_2\text{D}_4\text{Cl}_2$ at this temperature shows 11 resonances (Supporting Information, Figure S9), similar to the spectrum in CD_3CN at 343 K, shown in Figure 3. Taking all these observations together, we can conclude that in noncoordinating solvents such as CD_2Cl_2 or $1,2\text{-C}_2\text{D}_4\text{Cl}_2$, the five-coordinate complex $[\text{Fe}(\mathbf{1})](\text{OTf})_2$ is the dominant species at high temperature ($T > 273 \text{ K}$), which corresponds to the solid state structure obtained from a $\text{CH}_2\text{Cl}_2/\text{Et}_2\text{O}$ solution at room temperature (Figure 2, right). At low temperature, the triflate anions are coordinated and generate the seven-coordinate bis(triflate) complex $[\text{Fe}(\mathbf{1})(\text{OTf})_2]$ according to the equi-

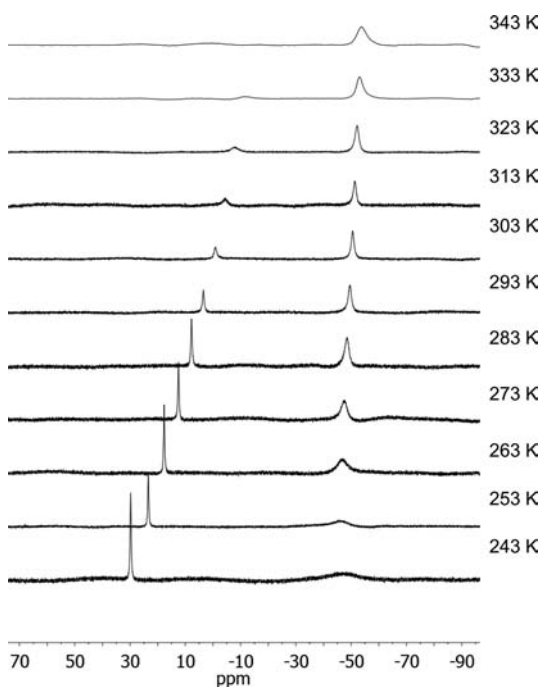
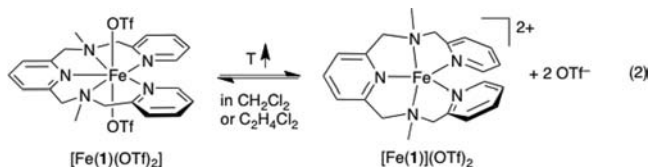


Figure 6. VT ^{19}F NMR spectra in the temperature range from 243 to 343 K for $[\text{Fe}(\mathbf{1})](\text{OTf})_2$ in $1,2\text{-C}_2\text{D}_4\text{Cl}_2$.

rium shown in eq 2. Changes in line widths of the ^{19}F NMR signals are related to the rate of triflate exchange in these



complexes, as was observed in similar iron(II) bis(triflate) complexes with tetradentate ligands.³³

The ^1H NMR spectrum for complex $[\text{Fe}(\mathbf{1})](\text{ClO}_4)_2$ in $1,2\text{-C}_2\text{D}_4\text{Cl}_2$ shows approximately 11 main signals at 343 K, similar to the spectrum in CD_3CN at 343 K, which corresponds to the five-coordinate complex $[\text{Fe}(\mathbf{1})](\text{ClO}_4)_2$ (see Supporting Information, Figure S13). Lowering the temperature results in a broadening of the signals and loss of intensity, probably because of poor solubility of the complex caused by self-association and the inability of the perchlorate anions to coordinate effectively to the iron(II) center.

Magnetic Susceptibility and Cyclic Voltammetry Measurements. The magnetic moments (μ_{eff}) for all complexes $[\text{Fe}(\mathbf{1})\text{Br}_2]$, $[\text{Fe}(\mathbf{1})](\text{OTf})_2$, $[\text{Fe}(\mathbf{1})](\text{CH}_3\text{CN})_2(\text{ClO}_4)_2$ and $[\text{Fe}(\mathbf{1})](\text{CH}_3\text{CN})_2(\text{SbF}_6)_2$ have been determined in CD_3CN solution over the temperature range from 233 to 343 K using the Evans' NMR method (see Supporting Information). Values between 5.0 and $5.5 \mu_{\text{B}}$ were measured for μ_{eff} over the entire temperature range, which are consistent with high spin d^6 iron(II) complexes ($S = 2$), whose μ_{eff} values range typically between 5.1 and $5.7 \mu_{\text{B}}$.⁹ Seven-coordinate *PBPY-7* and five-coordinate *TBPY-5* complexes are normally high spin and consequently, VT magnetic moment measurements cannot be used to characterize the 7–5 coordination equilibrium, unlike the *OC-6/SP-4* and *SP-4/T-4* coordination equilibria for nickel(II) complexes. Cyclic voltammetry measurements have been carried out in acetonitrile at 298 K. At this temperature, both seven- and five-coordinate complexes $[\text{Fe}(\mathbf{1})](\text{OTf})_2$ and $[\text{Fe}(\mathbf{1})](\text{OTf})_2$ are present, but only one signal with a half-potential of 0.99 V (vs SCE) for the $\text{Fe}(\text{II})/\text{Fe}(\text{III})$ redox couple was observed (see Supporting Information, Figure S22).

UV–vis Spectroscopy. VT UV–vis spectra of $[\text{Fe}(\mathbf{1})](\text{OTf})_2$, measured in $1,2\text{-C}_2\text{H}_4\text{Cl}_2$ (3 mM) over the temperature range from 233 to 333 K, are shown in Figure 7. At 233 K, an intraligand $\pi\text{-}\pi^*$ absorption is observed at 260 nm ($\epsilon = 7800 \text{ M}^{-1} \text{ cm}^{-1}$) and a broad metal-pyridine metal-to-ligand charge-transfer (MLCT) transition at 374 nm ($\epsilon = 900 \text{ M}^{-1} \text{ cm}^{-1}$). When the temperature is increased, the intensity of these bands decreases, and two new peaks appear at 261 nm ($\epsilon = 7500 \text{ M}^{-1} \text{ cm}^{-1}$) and 361 nm ($\epsilon = 800 \text{ M}^{-1} \text{ cm}^{-1}$). Two

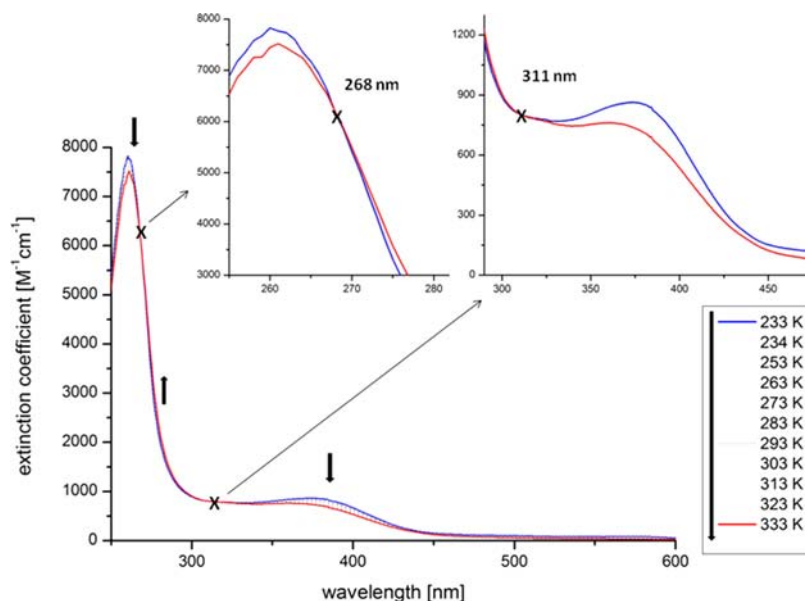
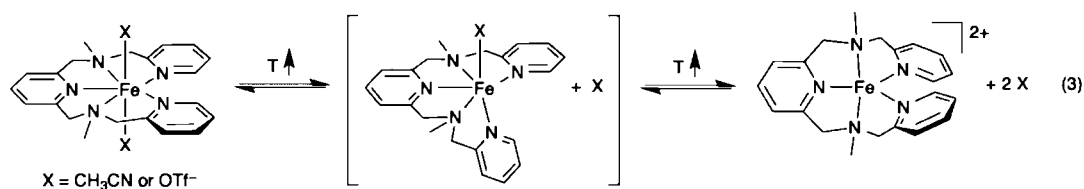


Figure 7. VT-UV–vis spectra of $[\text{Fe}(\mathbf{1})](\text{OTf})_2$ in $1,2\text{-C}_2\text{H}_4\text{Cl}_2$ (3 mM).



isobestic points are clearly observable at 268 and 311 nm, which is consistent with the proposed interconversion between two complexes of the 7–5 coordination equilibrium, as shown in eq 2.¹¹

The VT UV–vis spectra of $[\text{Fe}(\mathbf{1})](\text{OTf})_2$ recorded in CH_3CN (2 mM) show a similar, but less pronounced behavior (see Supporting Information, Figure S14). No evidence for any intermediate species has been observed in any of these measurements. The thermodynamic parameters have been determined by the van't Hoff plot of $\ln K$ versus $1/T$ and were found to be $\Delta H^\circ = 21.6 \pm 1.7 \text{ kJ mol}^{-1}$ and $\Delta S^\circ = 44 \pm 6 \text{ J K}^{-1} \text{ mol}^{-1}$ in CH_3CN (2 mM) and $\Delta H^\circ = 21.6 \pm 2.5 \text{ kJ mol}^{-1}$ and $\Delta S^\circ = 53 \pm 9 \text{ J K}^{-1} \text{ mol}^{-1}$ in $1,2\text{-C}_2\text{H}_4\text{Cl}_2$ (3 mM) (see Supporting Information, Figures S18 and S19 and Table S1). The enthalpy values are comparable to the value of $\Delta H^\circ = 25.1 \pm 1.1 \text{ kJ mol}^{-1}$ determined by NMR spectroscopy in acetonitrile, but the entropy values are somewhat lower (c.f. $\Delta S^\circ = 91 \pm 4 \text{ J K}^{-1} \text{ mol}^{-1}$ determined by NMR). The entropy values determined by UV–vis spectroscopy are less accurate because of the relatively small changes in the spectra and the determination from the intercept of the $\ln K$ versus $1/T$ graph. A comparable value of $\Delta S^\circ = 52 \pm 8 \text{ J K}^{-1} \text{ mol}^{-1}$ was measured for the OC-6/SP-4 equilibrium between $[\text{Ni}(\text{cyclam})\text{-(CH}_3\text{CN)}_2]^{2+}$ and $[\text{Ni}(\text{cyclam})]^{2+}$, which was also determined by VT UV–vis spectroscopy.¹¹

DISCUSSION

The interconversion between octahedral and square planar complexes in OC-6/SP-4 equilibria is generally very fast, with typical rate values of $10^4\text{--}10^6 \text{ s}^{-1}$.^{10,34,35} The planar-tetrahedral SP-4/T-4 coordination equilibria of nickel(II) complexes are equally very fast, typically in the order of $10^5\text{--}10^6 \text{ s}^{-1}$.⁷ Individual ^1H NMR spectra for the six-coordinate or four-coordinate complexes are normally not observed, and the signals are exchange averaged, despite fast relaxation times due to the paramagnetism. However, for certain dihalo diphosphine nickel(II) complexes, separate signals for both complexes could be observed at low temperatures, and VT NMR studies have allowed kinetic parameters to be determined.^{36–38}

In the 7–5 coordination equilibrium seen here, distinct signals are observed in the ^1H NMR spectra for the seven-coordinate PBPY-7 complex at low temperature and for the five-coordinate TBPY-5 complex at high temperature. No coalescence of the signals is observed, which suggests that the rate of interconversion must be much slower than the rate of relaxation. Because of the paramagnetic nature of both iron(II) complexes, relaxation times are fast, typically in the order of milliseconds.³⁹ This indicates that the rate of interconversion between the seven- and five-coordinate iron(II) complexes must be much slower than these relaxation times, probably in the order of seconds. The increase in the line width of the ^{19}F NMR signal for non-coordinated triflate above 333 K (see Figure 6), suggests that the rate of triflate exchange becomes comparable to the NMR time scale. Kinetic measurements will be needed in the future to determine the exact rates for these

reactions. A likely reason for the slow rate of exchange between the seven- and five-coordinate complexes seen here, is that the conformational rearrangement of the pentadentate ligand is energetically more demanding compared to the rearrangement in 6–4 coordination equilibria.

The OC-6/SP-4 equilibrium in nickel(II) complexes follows a dissociative mechanism via a five-coordinate intermediate.⁴⁰ The five-coordinate intermediate is identical to that proposed for ligand exchange at an octahedral metal complex.³⁵ Similarly, the reverse reaction, for example the addition of pyridine to four-coordinate nickel(II) complexes has been shown to proceed via a two-step process involving a five-coordinate intermediate. Measurements of the equilibrium constants revealed that $K_{4-5} \ll K_{5-6}$, and the five-coordinate intermediates are therefore rarely observable.^{7,41,42} Evidence for the existence of such intermediates has come from the isolation and characterization of paramagnetic five-coordinate nickel(II) complexes with pentadentate ligands, which react with pyridine to form six-coordinate octahedral nickel(II) complexes.^{40,43} Recent DFT calculations have shown that the addition of pyridine to the square planar four-coordinate complex $[\text{Ni}(\text{acac})_2]$ proceeds via an associative mechanism, whereby the singlet–triplet conversion occurs during the first addition of pyridine which is rate-determining, whereas the addition of the second pyridine ligand is without an energy barrier.¹⁷

Substitution reactions of seven-coordinate transition metal complexes generally operate via a dissociative mechanism, involving a six-coordinate intermediate.⁴⁴ We propose at this stage that the 7–5 equilibrium seen here proceeds by a two stage process via a six-coordinate intermediate such as $[\text{Fe}(\mathbf{1})(\text{CH}_3\text{CN})](\text{OTf})_2$ or $[\text{Fe}(\mathbf{1})(\text{OTf})](\text{OTf})$ (eq 3). So far, we have been unable to detect such six-coordinate intermediates by NMR or UV–vis spectroscopy. In the case of acetonitrile as the additional donor, the complex $[\text{Fe}(\mathbf{1})(\text{CH}_3\text{CN})]^{2+}$ is most likely a low spin or a spin crossover complex at room temperature, similar to other octahedral iron(II) complexes with a comparable ligand field consisting of three pyridine donors, two amines, and one acetonitrile donor, for example in $[\text{Fe}(\text{TPMEN})(\text{CH}_3\text{CN})]^{2+}$ (TPMEN = tris-(pyridylmethyl)-*N*-methylethylenediamine).⁴⁵ A low spin intermediate would require two spin transitions along the 7–6–5 conversion pathway with the associated energy barriers, and it may therefore be energetically favorable for an intermediate six-coordinate HS iron(II) complex to dissociate another ligand to form the five-coordinate HS complex, rather than undergo a spin transition. A LS octahedral iron(II) d^6 intermediate would be kinetically inert and reluctant to undergo further ligand dissociation and therefore should be detectable. Indeed, two examples of a related reversible ligand dissociation in an equilibrium between a HS seven-coordinate iron(II) and a LS six-coordinate iron(II) complex have been observed in the solid state and in solution.^{46,47}

Noteworthy in this context are two related studies. First, Kim and co-workers reported a related macrocyclic and potentially

hexadentate ligand, which gave a five-coordinate iron(II) complex with a similar structure as $[\text{Fe}(\mathbf{1})](\text{OTf})_2$.⁴⁸ Coordination of an additional ligand such as acetonitrile to give a six-coordinate complex was not observed. Rearrangement of the five-coordinate complex to give a seven-coordinate complex is probably inhibited by the constraints imposed by the macrocyclic ligand. A second relevant study was reported by Ball, Colbran, and co-workers on a related iron(II) complex with a heptadentate pyridyldiamine ligand with four pyridylmethyl arms.⁴⁹ The seven-coordinate *PBPY*-7 iron(II) complex undergoes dynamic fluxional behavior at higher temperatures, resulting in a simultaneous exchange of the equatorial and axial pyridine ligands, which is assumed to occur via a six-coordinate intermediate with one non-coordinated pyridylmethyl arm. A five-coordinate iron(II) complex with two non-coordinated pyridylmethyl arms was not observed, which is understandable as the formation of the five-coordinate complex seen here is entropically favored by the loss of the two axial ligands.

CONCLUSION

The pentadentate ligand **1** generates iron(II) complexes that display a coordination equilibrium in solution. While unequivocal evidence is yet to be obtained, the results presented here suggest that at low temperature, in the presence of coordinating ligands such as CH_3CN or triflate anions, the formation of a seven-coordinate iron(II) complex with *PBPY*-7 geometry is observed, whereas at high temperature a five-coordinate complex with *TBPY*-5 geometry is formed upon loss of two ligands. VT NMR and UV-vis studies have provided evidence for the proposed 7–5 equilibrium and the thermodynamic parameters have been determined as $\Delta H^\circ = 25.1 \pm 1.1 \text{ kJ mol}^{-1}$ and $\Delta S^\circ = 91 \pm 4 \text{ J K}^{-1} \text{ mol}^{-1}$ by NMR spectroscopy in acetonitrile and as $\Delta H^\circ = 21.6 \pm 1.7 \text{ kJ mol}^{-1}$ and $\Delta S^\circ = 44 \pm 6 \text{ J K}^{-1} \text{ mol}^{-1}$ in acetonitrile by UV-vis spectroscopy. The 7–5 equilibrium is related to the 6–4 coordination equilibrium, which is well established for nickel(II) complexes. Kinetic measurements will be needed to establish the rate of the 7–5 interconversions, which appear to be much slower than 6–4 and 4–4 coordination equilibria.

The discovery of the first example of a 7–5 coordination equilibrium generates several new directions. It is unlikely that the iron(II) complexes shown here are unique, and other metal complexes with other ligands and metals in different oxidation states may also undergo a 7–5 coordination equilibrium. Furthermore, it now appears that the 6–4 and 4–4 coordination equilibria discovered 50 years ago are not unique, which raises the question whether other coordination equilibria may exist, for example 5–3 or 8–6? Indeed, an example for an 8–6 equilibrium has been suggested by Hagen between a cubic eight-coordinate iron(II) complex and an octahedral iron(II) complex, which will need further investigation.⁵⁰

EXPERIMENTAL SECTION

2,6-Bis[(methyl(2-pyridylmethyl)amino)methyl]pyridine 1. 2,6-Pyridinedicarboxaldehyde (660 mg, 4.91 mmol) was dissolved in dichloromethane (20 mL) and methyl(2-pyridylmethyl)amine (1.20 g, 9.82 mmol) added. The yellow reaction mixture was stirred at room temperature overnight. Sodium triacetoxyborohydride (3.12 g, 14.73 mmol) was added, and the mixture was stirred overnight at room temperature. To quench excess of triacetoxyborohydride and reach a pH value of about 8, an aqueous saturated solution of sodium hydrogencarbonate (10 mL) was added slowly. The aqueous phase was extracted three times with dichloromethane (3 × 20 mL). The organic phases were combined, dried over MgSO_4 , filtered, and the

solvent was removed under reduced pressure. The crude product was washed with hexane and small amounts of diethyl ether. After drying under vacuum, the product was isolated as viscous yellow oil. Yield: 1.49 g (87%). ¹H NMR (CDCl_3 , 400 MHz): δ (ppm) = 8.54 (d, $J = 4.8 \text{ Hz}$, 2H, 6-PyH), 7.65 (t, $J = 7.7 \text{ Hz}$, 3H, 4-PyH and PyH_p), 7.52 (d, $J = 7.8 \text{ Hz}$, 2H, 3-PyH), 7.42 (d, $J = 7.7 \text{ Hz}$, 2H, PyH_m), 7.15 (t, $J = 6.5 \text{ Hz}$, 2H, 5-PyH), 3.78 (s, 4H, 2 × NCH₂), 3.77 (s, 4H, 2 × NCH₂), 2.31 (s, 6H, 2 × NCH₃). ¹³C NMR (CDCl_3 , 101 MHz): δ (ppm) = 159.40, 158.61, 149.18, 136.84, 136.40, 123.06, 121.93, 121.08, 63.64, 63.50, 42.84. ESI-MS: $m/z = 370$ [$\text{M}+\text{Na}$]⁺, 348 [$\text{M}+\text{H}$]⁺.

[Fe(1)Br₂]. Ligand **1** (356.5 mg, 1.03 mmol) was dried under vacuum for about 2 h and dissolved in abs. acetonitrile (10 mL). Under inert atmosphere, the solution of **1** was added to a suspension of FeBr_2 (221.3 mg, 1.03 mmol) in abs. acetonitrile (10 mL). The reaction mixture was heated to 70 °C and stirred overnight. The solvent was then removed under reduced pressure to about a third of the volume. The complex was isolated by precipitation with diethyl ether and dried under vacuum. Complex $[\text{Fe}(\mathbf{1})\text{Br}_2]$ was obtained as yellow solid. Yield: 600 mg (60%). Crystals suitable for X-ray analysis were grown at room temperature by slow-diffusion from a acetonitrile solution layered with diethyl ether. ¹H NMR (CD_3CN , 400 MHz, all peaks appear as broad singlets): δ (ppm) = 133.71, 101.65, 88.71, 72.88, 54.52, 50.90, 48.47, 47.40, 28.84, 17.08, 12.61, 9.87, –8.09. MS-FAB $m/z = 484$ [$\text{M}-\text{Br}$]⁺. Anal. Calcd. (found) for $\text{C}_{21}\text{H}_{25}\text{Br}_2\text{FeN}_5$: %C 44.79 (44.59), %H 4.48 (4.33), %N 12.44 (12.31). UV-vis (CH_3CN): λ_{max} (nm) 383, 260, 218. $\mu_{\text{eff}}(\text{CD}_2\text{Cl}_2) = 5.33 \mu_{\text{B}}$, $\mu_{\text{eff}}(\text{CD}_3\text{CN}) = 5.16 \mu_{\text{B}}$.

[Fe(1)](OTf)₂. $[\text{Fe}(\mathbf{1})\text{Br}_2]$ (200.00 mg, 0.36 mmol) and silver triflate (185.00 mg, 0.72 mmol) were placed into a Schlenk flask and dissolved in abs. dichloromethane. The reaction mixture was stirred overnight at room temperature. The gray precipitate (AgBr) formed was removed by filtration. The remaining pale yellow solution was concentrated to about one-third of the volume. Afterwards, pentane was added to precipitate the product as yellow to light brown oil. The oil was dried under vacuum yielding complex $[\text{Fe}(\mathbf{1})](\text{OTf})_2$ as yellow solid. Yield: 126.2 mg (50%). Crystals suitable for X-ray analysis were grown at room temperature by slow-diffusion from a dichloromethane solution layered with pentane. ¹H NMR (CD_3CN , 400 MHz, all peaks appear as broad singlets): δ (ppm) = 147.72, 130.74, 114.22, 110.12, 105.43, 99.29, 75.05, 73.21, 64.75, 63.02, 59.10, 56.05, 54.15, 53.04, 52.28, 36.91, 35.17, 30.46, 25.59, 24.77, 6.60, 5.66, –1.29, –3.16, –4.13. ¹⁹F NMR (CD_3CN , 376 MHz, all peaks appear as broad singlets): δ (ppm) = –76.50. MS-FAB $m/z = 552$ [$\text{M}-\text{OTf}$]⁺. LSIMS $m/z = 552$ [$\text{M}-\text{OTf}$]⁺. Anal. Calcd. (found) for $\text{C}_{23}\text{H}_{25}\text{F}_6\text{FeN}_5\text{O}_6\text{S}_2$: %C 39.38 (39.37), %H 3.59 (3.52), %N 9.98 (9.79). UV-vis (CH_3CN): λ_{max} (nm) 359, 260, 214. $\mu_{\text{eff}}(\text{CD}_3\text{CN}) = 5.35 \mu_{\text{B}}$, $\mu_{\text{eff}}(\text{CD}_2\text{Cl}_2) = 5.27 \mu_{\text{B}}$.

[Fe(1)](SbF₆)₂. Ligand **1** (107.9 mg, 0.31 mmol) was dried under vacuum for about 2 h and dissolved in abs. acetonitrile (15 mL). Under inert atmosphere, the solution of **1** was added to a solution of $[\text{Fe}(\text{CH}_3\text{CN})_6](\text{SbF}_6)_2$ (239.8 mg, 0.31 mmol) in abs. acetonitrile (15 mL). Upon addition of the ligand solution the reaction mixture turned intense orange, and the mixture was stirred at room temperature overnight. The next day the solvent was removed under reduced pressure to about a third of the volume. The complex was isolated by precipitation with diethyl ether and dried under vacuum. Complex $[\text{Fe}(\mathbf{1})](\text{SbF}_6)_2$ was obtained as an orange solid. Yield: 205.4 mg (70%). This complex is only sparingly soluble in chlorinated solvents. ¹H NMR (CD_3CN , 400 MHz, all peaks appear as broad singlets): δ (ppm) = 147.91, 130.57, 121.05, 115.38, 110.50, 99.35, 75.02, 72.99, 64.83, 62.57, 60.21, 59.47, 58.93, 55.81, 54.29, 53.20, 52.89, 37.02, 35.27, 30.41, 25.60, 5.43, –1.38, –3.24, –4.25. ¹⁹F NMR (CD_3CN , 376 MHz, all peaks appear broadened): δ (ppm) = –121.82 (superposition of a sextet due to ¹²¹SbF₆[–] ($J_{\text{F}-121\text{Sb}} = 1057 \text{ Hz}$) and an octet due to ¹²³SbF₆[–] ($J_{\text{F}-123\text{Sb}} = 1936 \text{ Hz}$). LSIMS $m/z = 638$ [$\text{M}-\text{SbF}_6$]⁺. HRESI $m/z = 638.0413$ [$\text{M}-\text{SbF}_6$]⁺, 201.5767 [M]²⁺. Anal. Calcd. (found) for $\text{C}_{21}\text{H}_{25}\text{F}_{12}\text{FeN}_5\text{Sb}_2$: %C 28.83 (28.90), %H 2.88 (2.75), %N 8.01 (8.04). $\mu_{\text{eff}}(\text{CD}_3\text{CN}) = 5.0 \mu_{\text{B}}$.

[Fe(1)](ClO₄)₂. Ligand **1** (250.4 mg, 0.72 mmol) was dried under vacuum for about 2 h. Under inert atmosphere, $\text{Fe}(\text{ClO}_4)_2 \cdot \text{H}_2\text{O}$

(184.0 mg, 0.72 mmol) was dissolved in abs. acetonitrile (10 mL) and subsequently added to **1**. Upon addition of the metal precursor solution the reaction mixture turned dark yellow. The mixture was stirred at room temperature for 3 h after which abs. diethyl ether (30 mL) was added. Upon cooling the complex precipitated as brown oil. The oil was dried under reduced pressure yielding complex $[\text{Fe}(\text{I})(\text{CH}_3\text{CN})_2](\text{ClO}_4)_2$ as yellow solid. Yield: 180.00 mg (28%). Crystals suitable for X-ray analysis were grown by slow-diffusion from an acetonitrile solution layered with diethyl ether. $^1\text{H NMR}$ (CD_3CN , 400 MHz, all peaks appear as broad singlets): δ (ppm) = 145.22, 127.97, 114.11, 108.27, 106.35, 103.59, 97.89, 73.87, 72.62, 71.20, 70.35, 64.25, 62.21, 58.42, 54.92, 53.48, 52.09, 36.66, 34.87, 34.36, 30.73, 25.46, 23.90, 6.10, 5.33 -1.25 , -2.33 , -2.89 , -3.86 . MS-FAB $m/z = 502$ $[\text{M}-\text{ClO}_4]^+$. μ_{eff} (CD_3CN) = 5.31 μ_{B} .

■ ASSOCIATED CONTENT

📄 Supporting Information

X-ray crystallographic files in CIF format for all complexes and experimental details regarding magnetic susceptibility measurements and spectroscopic procedures. This material is available free of charge via the Internet at <http://pubs.acs.org>.

■ AUTHOR INFORMATION

Corresponding Author

*E-mail: g.britovsek@imperial.ac.uk. Phone: +44-(0)-20-75945863. Fax: +44-(0)-20-75945804.

Notes

The authors declare no competing financial interest.

■ ACKNOWLEDGMENTS

We are grateful to EPSRC and Unilever for financial support. We thank Prof. James Beattie for helpful discussions.

■ REFERENCES

- (1) Hartshorn, R. M.; Hey-Hawkins, E.; Kalio, R.; Leigh, G. J. *Pure Appl. Chem.* **2007**, *79*, 1779–1799.
- (2) Dürr, K.; Jux, N.; Zahl, A.; van Eldik, R.; Ivanovic-Burmazovic, I. *Inorg. Chem.* **2010**, *49*, 11254–11260.
- (3) Berry, R. S. *J. Chem. Phys.* **1960**, *32*, 933–938.
- (4) Muettterties, E. L.; Guggenberger, L. J. *J. Am. Chem. Soc.* **1974**, *96*, 1748–1756.
- (5) Holm, R. H.; O'Connor, M. J. *Prog. Inorg. Chem.* **1971**, *14*, 241–401.
- (6) Sacconi, L.; Paoletti, P.; Ciampolini, M. *J. Am. Chem. Soc.* **1963**, *85*, 411–416.
- (7) Knoch, R.; Elias, H.; Paulus, H. *Inorg. Chem.* **1995**, *34*, 4032–4040.
- (8) Mori, Y.; Shirase, H.; Fukuda, Y. *Bull. Chem. Soc. Jpn.* **2008**, *81*, 1108–1115.
- (9) Barefield, E. K.; Busch, D. H.; Nelson, S. M. *Quart. Rev. Chem. Soc.* **1968**, *22*, 457–498.
- (10) Segla, P.; Elias, H. *Inorg. Chim. Acta* **1988**, *149*, 259–264.
- (11) Boiocchi, M.; Fabbri, L.; Foti, F.; Vázquez, M. *Dalton Trans.* **2004**, 2616–2620.
- (12) Swaddle, T. W.; Fabes, L. *Can. J. Chem.* **1980**, *58*, 1418–1426.
- (13) Chakravorty, A.; Fennessy, J. P.; Holm, R. H. *Inorg. Chem.* **1965**, *4*, 26–33.
- (14) Schumann, M.; Elias, H. *Inorg. Chem.* **1985**, *24*, 3187–3192.
- (15) Beattie, J. K. *Adv. Inorg. Chem.* **1988**, *32*, 1–53.
- (16) Coates, J. H.; Hadi, D. A.; Lincoln, S. F.; Dodgen, H. W.; Hunt, J. P. *Inorg. Chem.* **1981**, *20*, 707–711.
- (17) Starikov, A. G.; Minyaev, R. M.; Starikova, A. A.; Minkin, V. I. *Russ. J. Coord. Chem.* **2010**, *36*, 597–604.
- (18) Schollenberger, M.; Nuber, B.; Ziegler, M. L. *Angew. Chem., Int. Ed.* **1992**, *31*, 350–351.

- (19) Christie, K. O.; Curtis, E. C.; Dixon, D. A.; Mercier, H. P.; Sanders, J. C. P.; Schrobilgen, G. J. *J. Am. Chem. Soc.* **1991**, *113*, 3351–3361.
- (20) Stubbe, J.; Kozarich, J. W. *Chem. Rev.* **1987**, *87*, 1107–1136.
- (21) Salvemini, D.; Wang, Z.-Q.; Zweier, J. L.; Samouilov, A.; Macarthur, H.; Misko, T. P.; Currie, M. G.; Cuzzocrea, S.; Sikorski, J. A.; Riley, D. P. *Science* **1999**, *286*, 304–306.
- (22) Riley, D. P. *Chem. Rev.* **1999**, *99*, 2573–2587.
- (23) Darbre, T.; Dubs, C.; Rusanov, E.; Stoeckli-Evans, H. *Eur. J. Inorg. Chem.* **2002**, 3284–3291.
- (24) Gruenwedel, D. W. *Inorg. Chem.* **1968**, *7*, 495–501.
- (25) Newkome, G. R.; Gupta, V. K.; Fronczek, F. R.; Pappalardo, S. *Inorg. Chem.* **1984**, *23*, 2400–2408.
- (26) Casanova, D.; Alemany, P.; Boffill, J. M.; Alvarez, S. *Chem.—Eur. J.* **2003**, *9*, 1281–1295.
- (27) Craig, G. A.; Barrios, L. A.; Costa, J. S.; Roubeau, O.; Ruiz, E.; Teat, S. J.; Wilson, C. C.; Thomas, L.; Aromi, G. *Dalton Trans.* **2010**, *39*, 4874–4881.
- (28) Ivanovic-Burmazovic, I.; Andjelkovic, K. *Adv. Inorg. Chem.* **2004**, *55*, 315–360.
- (29) Wester, D.; Palenik, G. J. *J. Am. Chem. Soc.* **1973**, *95*, 6505–6506.
- (30) Koenig, E.; Ritter, G.; Dengler, J.; Nelson, S. M. *Inorg. Chem.* **1987**, *26*, 3582–3588.
- (31) Addison, A. W.; Nageswara Rao, T.; Reedijk, J.; van Rijn, J.; Verschoor, G. C. *J. Chem. Soc., Dalton Trans.* **1984**, 1349–1356.
- (32) Chai, J.-D.; Head-Gordon, M. *Phys. Chem. Chem. Phys.* **2008**, *10*, 6615–6620.
- (33) England, J.; Gondhia, R.; Bigorra-Lopez, L.; Petersen, A. R.; White, A. J. P.; Britovsek, G. J. P. *Dalton Trans.* **2009**, 5319–5334.
- (34) Godfrey, A. F.; Beattie, J. K. *Inorg. Chem.* **1983**, *22*, 37943798.
- (35) Cusumano, M. *J. Chem. Soc., Dalton Trans.* **1976**, 2133–2136.
- (36) La Mar, G. N.; Sherman, E. O. *J. Am. Chem. Soc.* **1970**, *92*, 2691–2699.
- (37) Pignolet, L. H.; Horrocks, W. D., Jr.; Holm, R. H. *J. Am. Chem. Soc.* **1970**, *92*, 1855–1863.
- (38) Que, L., Jr.; Pignolet, L. H. *Inorg. Chem.* **1973**, *12*, 156–163.
- (39) Drago, R. S. *Physical Methods for Chemists*; Saunders College: London, U.K., 1992.
- (40) Thwaites, J. D.; Bertini, I.; Sacconi, L. *Inorg. Chem.* **1966**, *5*, 1036–1041.
- (41) Dakternieks, D. R.; Graddon, D. P. *Aust. J. Chem.* **1973**, *26*, 2379–2389.
- (42) Schumann, M.; von Holtum, A.; Wannowius, K. J.; Elias, H. *Inorg. Chem.* **1982**, *21*, 606–612.
- (43) La Mar, G. N.; Sacconi, L. *J. Am. Chem. Soc.* **1967**, *89*, 2282–2291.
- (44) Dees, A.; Zahl, A.; Puchta, R.; van Eikema Hommes, N. J. R.; Heinemann, F. W.; Ivanovic-Burmazovic, I. *Inorg. Chem.* **2007**, *46*, 2459–2470.
- (45) Mialane, P.; Nivorjokine, A.; Pratiel, G.; Azéma, L.; Slany, M.; Godde, F.; Simaan, A. J.; Banse, F.; Kargar-Grisel, T.; Bouchoux, G.; Sinton, J.; Horner, O.; Guilhem, J.; Tchertanova, L.; Meunier, B.; Girerd, J.-J. *Inorg. Chem.* **1999**, *38*, 1085–1092.
- (46) Brady, C.; Callaghan, P. L.; Ciunik, Z.; Coates, C. G.; Døssing, A.; Hazell, A.; McGarvey, J. J.; Schenker, S.; Toftlund, H.; Trautwein, A. X.; Winkler, H.; Wolny, J. A. *Inorg. Chem.* **2004**, *43*, 4289–4299.
- (47) Guionneau, P.; Le Gac, F.; Kaiba, A.; Sánchez Costa, J.; Chasseau, D.; Létard, J.-F. *Chem. Commun.* **2007**, 3723–3725.
- (48) You, M.; Seo, M. S.; Kim, K. M.; Nam, W.; Kim, J. *Bull. Korean Chem. Soc.* **2006**, *27*, 1140–1144.
- (49) Lonnon, D. G.; Ball, G. E.; Taylor, I.; Craig, D. C.; Colbran, S. B. *Inorg. Chem.* **2009**, *48*, 4863–4872.
- (50) Diebold, A.; Hagen, K. S. *Inorg. Chem.* **1998**, *37*, 215–223.